Int J Adv Manuf Technol (2018) 94:85–103
DOI 10.1007/s00170-017-0808-x

ORIGINAL ARTICLE

Performance study of multilayer carbide tool in high-speed turning of API 5L X70 pipeline steel using a cold air system

Étory Madrilles Arruda[1] · **Lincoln Cardoso Brandão**[1]

Received: 6 March 2017 / Accepted: 14 July 2017 / Published online: 5 August 2017

Abstract Turning is the most widespread manufacturing process in the industry due to its high flexibility in machining for simple and complex parts. The study of surface roughness and tool wear are the main responses in the machining processes, mainly in the turning process. The great challenge in the modern industry is to increase the productivity with time reduction without decreasing the quality and raising the costs of the products. In this study, seamless tubular workpieces of API 5L X70 steel were used to define the surface roughness and the tool wear. The responses were tool life with VB_{max} greater than or equal to 0.3 mm and lowest surface roughness value in machining tests using a dry and cold air system. The results demonstrated that the use of high cutting speeds provided a significant reduction in tool life. The use of the cold air system provided a good increase in tool life for the traditional speed. On the other hand, the turning process with the cold air system and high-speed cutting reduced the tool life significantly. Finally, the increase in VB_{max} provided the increase in surface roughness of the workpieces. Concerning the cutting speed, it was found that their increase provided a reduction in the cutting efforts, both in dry experiments and in experiments with the cold air system.

Keywords High-speed turning · Wear · Cold air · Surface roughness

✉ Lincoln Cardoso Brandão
lincoln@ufsj.edu.br

Étory Madrilles Arruda
etory@msn.com

[1] Department of Mechanical Engineering, Center for Innovation in Sustainable Manufacturing, Federal University of São João del-Rei, Praça Frei Orlando, 170, centro, 36, São João del Rei 307-352, Brazil

1 Introduction

Turning is the most widespread manufacturing process in the industry due to its flexibility in machining simple parts or mechanical components with more complex geometries. Surface roughness and tool wear are the main responses in the machining processes to define the efficiency of the manufacturing sector [1–3]. According to Kumar and Sahoo [4], carbide tools were developed in 1928 aiming to achieve high production rates and were firstly used in the turning process. Carbide tools have specific physical characteristics that provide not only low thermal conductivity but also the capability to quickly dissipate the heat generated during the machining process [5].

The great challenge in the modern industry is to increase the productivity with time reduction without decreasing the quality and raising the costs of the products. High-speed machining has been the philosophy used in the last 20 years to promote this paradigm break. However, what does high-speed in machining mean? This is an interesting question, because the cutting speed in machining processes can vary according to the process, since each machining process has its specific characteristics that must be considered. On the other hand, the machined materials have different structures that should also be considered during the manufacturing strategy.

According to Katama and Obikawa [6], the improvement of tool lives in machining processes has occurred due to the production of several types of coatings for machining tools. The authors studied the use of the minimum quantity lubrication (MQL) system in turning of Inconel 718 and three selected coatings. The results showed that the $TiCN/Al_2O_3/TiN$ coating had the best performance together with the use of a MQL coolant system due to the thermal barrier promoted by the Al_2O_3 layer. However, the increase by 50% in cutting speed decreased the tool lives drastically. The rise of

temperature in machining due to the increase of cutting speed can be considered a great challenge because it reduces the tool life significantly [7].

Several authors have studied high-speed machining in the last decades. However, the main focuses are on the turning and the milling processes due to their great application in the industry and their elevated flexibility. The turning process is a classical machining process with a large application because it not only enables the manufacture of simple geometries with high precision but also produces preforms for later steps in shop floors [8–10]. On the other hand, the milling process produces complex geometries such as moulds, dies, and gears. Usually, the milling of moulds and dies is performed in hardened steels reducing the manufacturing steps [11–13].

Independent of the manufacturing process type and its application, the quality is the most important factor and it depends on the correct choice of the machining input parameters. Surface roughness is a classical parameter used as a response to control the quality of products. The current focus in the industry is to optimize the surface roughness because it has a direct influence on the mechanical component efficiency. Surface roughness influences several aspects of the machining processes such as tooling choice, assembly of components, and visual aspects of the pieces. Beno et al. [2] developed a methodology based on the surface roughness in order to stimulate the correct choice of inserts in process planning. According to the authors, the traditional patterns R_a, R_q, R_z, R_t, and R_p showed a linear relationship and the chip cross section showed a great influence on surface roughness.

Surface roughness has been used as an accurate response quality parameter in the last three decades. The great challenge is to predict surface roughness before the part was machined. Several authors developed methodologies in order to predict the surface roughness. Qehaja et al. [14] demonstrated that various cutting parameters could affect the surface roughness in dry turning of coated tungsten carbide inserts. The authors support that the feed rate seems to influence surface roughness more significantly than nose radius and cutting time. Upadhyay et al. [15] used the neural network technique and Pearson correlation to predict the surface roughness. The results showed that both models predicted the surface roughness with reasonable accuracy, making them suitable for process prediction.

However, the evolution of the tool wear can compromise the predictions of surface roughness because the geometry of the tool changes, with the occurrence of noise radius, chip breaker, and coating during the machining process due to the wear. These variations in tool geometry can collaborate with the increase of diffusion, attrition, and chipping mechanisms, changing randomly the surface roughness. All studies about tool wear are performed in parallel with surface roughness since the cutting tool geometry deteriorates and the surface roughness values of the workpiece can increase rapidly. It happens for instance, when carbide and ceramic tools are used [16, 17].

Considering the traditional cutting speeds in machining, the surface roughness behaviour has demonstrated a proportional increase of values when the tool wear rises [14, 18]. However, in some situations, surface roughness can increase or decrease simultaneously. Such characteristics showed a stochastic behaviour, which depends not only on nose radius and feed rate but also on other machining parameters such as material type, hardening, and cutting speed [19, 20]. Finally, it can be supported that the studies on high-speed cutting focused on wear and surface roughness are still modest, mainly due to the extensive number of materials and types of tools used in the industry. Also, it is hard to define correctly the values of high speed in machining processes.

Based on these considerations, in this study the tool wear for a specific pair tool/material (coated carbide insert and API 5L X70 steel) used in the world oil industry [21] was evaluated. The tool wear with conventional and high-speed cutting was recorded together with the surface roughness evolution. Furthermore, the upper limit for high-speed cutting was defined and fixed in the experimental tests.

2 Methodology

2.1 Tool wear tests

Experimental machining tests were carried out using a turning centre with 6000 rpm of spindle speed and 22.5 kW of main power. The turning centre was controlled by FANUC numerical control. Seamless tubular workpieces of API 5L X70 steel with yield strength of 694 MPa, tensile strength of 822 MPa, hardness of 45 HRC, external diameter of 200 mm, internal diameter of 150 mm, and length of 300 mm were used to define the surface roughness and the tool wear. The external diameter of 200 mm provided experiments with high-speed cutting without exceeding the maximum speed of the machine spindle. API 5L X70 is a specific steel used in oil exploration pipes with medium carbon and low chrome, as can be seen in Table 1.

However, considering high-strength and low-alloy steel, the presence of Cr, Mn, Mo, and Si and the high-speed cutting were decisive for the choice of the tooling used in experimental tests. Thus, a class of triangular inserts with code TNMG 160408-MF (GC 1125), produced by PVD process with WC grains sub-micron and thin double coating of TiAlN and $(AlCr)_2O_3$, was used in turning tests. Table 2 shows the chemical composition and the characteristics of the GC 1125 cutting tool. The tool holder with code DTJNL 2020K 16 was also used in turning tests.

The experiments were defined as finishing tests to study the surface quality of sleeves used in pipelines and tool wear.

Table 1 Chemical composition of API 5 L X70 steel

Chemical elements [% weight]								
C	Cr	Mn	Mo	Si	P	S	Fe	others
0.25	0.94	0.83	0.45	0.24	0.025	0.001	97.144	0.12

Figure 1 shows the setup used in experimental tests where it can be noticed that the use of the tailstock was necessary due to the great overhang of workpieces.

The flank wear (VB_{max}) was measured using an optical microscope Mitutoyo TM-500 with ×30 magnification. A Moticam 2300 camera attached to a computer and the microscope used the Motic Images Plus 2.0ML software to provide the acquisition and processing of the tool wear images. The criterion used as the end of tool life was VB_{max} greater than or equal to 0.3 mm. Thus, various cutting passes were performed until it reached VB_{max}. After each cutting pass, the tool was analysed in an optical microscope and VB_{max} was measured.

After the tool achieves the VB_{max} defined, the tool was analysed using scanning electron microscopy (SEM) and energy-dispersive X-ray spectroscopy (EDS) in order to define the types and mechanisms of wear of the cutting tools. For SEM and EDS, a microscope Hitachi TM3000 at a constant acceleration voltage of 15 kV was used. This microscope was assembled in a computer with TM3000 and QUANTAX 70 software.

Before performing SEM and EDS analysis, some traditional metallographic procedures were performed. The tools, one at a time, were placed in immersion in a nitric acid solution with a concentration of 33% in volume during 2 min, and then neutralized and cleaned with flowing water and dried with a hot air blower. Thus, the characterization of the types and active wear mechanisms in the cutting tools would be more detailed.

The turning tests were carried out using a cold air system to provide a comparison with the dry cut and to evaluate the cooling efficiency. The cold air system uses the vortex principle decreasing the environmental temperature to −5 °C. Brandão et al. [12] applied the same cooling system in finishing milling because the volume of the material removed in dies and moulds is smaller, as well as in finishing turning. Hence, the vortex system showed a high efficiency for cooling in the cutting region.

For the turning tests, a vortex tube positioned at 5 mm from the tool tip together with an air dehumidifier was used.

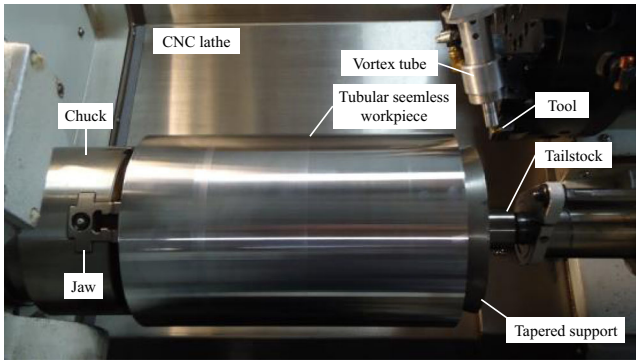

Fig. 1 Detail of the tool wear experiments

Besides, necessary for the experiments were a storage unit with a pressure regulator positioned in the vortex tube inlet and an air compressor. The air pressure in the vortex tube inlet was kept constant in 5.4 bars; the average temperature of the cold air was −5 °C, and it was measured at 5 mm from the air outlet nozzle. The experimental setup of the cold air system can be seen in Fig. 2.

The setup of the air dehumidifier, of the storage unit with pressure regulator, and of the position of the vortex tube was determined through preliminary tests. Using an acquisition board NI 9211 assembled on chassis NI cDAQ-9172, a thermocouple type k, and LabVIEW and Scilab software, it was possible to perform the acquisition and check the variation in cold air temperature in the vortex tube outlet at 0, 5, and 10 mm, as can be seen in Fig. 3. Furthermore, it was observed that the use of the air dehumidifier provided a decrease of cold air in the outlet temperature.

The high-speed concept is complex and depends on several parameters such as material, tooling, and, mainly, the machining process. High-speed tapping, for example, can be ten times lower than high-speed turning for the same material. On the other hand, high-speed turning in aluminium and its alloys can be ten times higher than high-speed turning of hardened steel. Based on this, preliminary tests were carried out to define the exact limit for high-speed turning in API 5L X70 steel with carbide tool.

According to preliminary tests, the maximum cutting speed was three times the recommended cutting speed by the tool supplier. Thus, the experimental tests were defined and carried out, according to Table 3, with a limit of three times the cutting speed recommended for the TNMG 160408-MF (GC 1125) inserts and an intermediate cutting speed.

Table 2 Chemical composition and characteristics of GC 1125 cutting tool

Substrate (% composition)			Density (g/cm^3)	Hardness (HV)	Coating thickness (μm)	
Co	WC	Cr_3C_2	14.40	1640	TiAlN	$(AlCr)_2O_3$
16.20	81.60	2.20			2.0	0.7

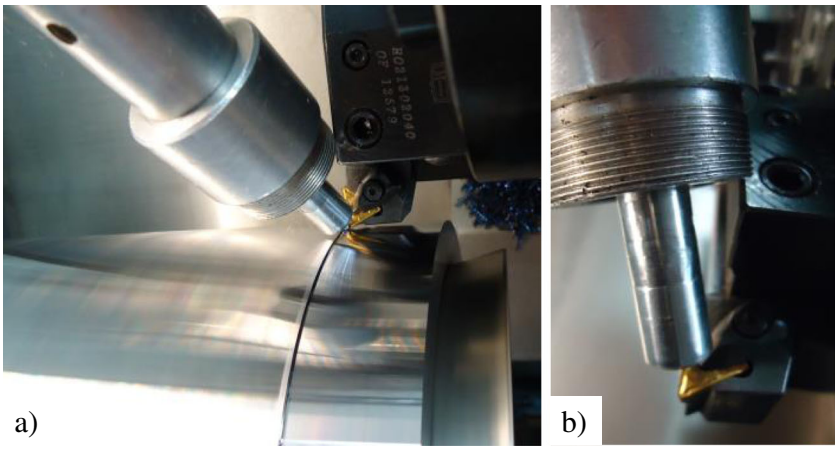

Fig. 2 **a** Turning with cold air system. **b** Details of vortex tube and cutting tool

2.2 Cutting effort measurements

In the study of cutting efforts, API 5L X70 workpieces with different dimensions were used. These workpieces corresponded to a cross section of the seamless tubular workpiece used in the experiments to measure surface roughness and tool wear. This specific workpiece was turned internally and externally and also turned in its outer diameter three grooves with width of 3 mm and depth of 10 mm, resulting in the configuration shown in Fig. 4a. Thus, the four shoulders with width of 8 mm and depth of 10 mm were used to carry out the cutting effort measurements.

2.3 Surface roughness measurements

The surface roughness with regard to average surface roughness (R_a) was measured using a surf tester Mitutoyo SJ-400 with a cutoff of 0.8 mm. Similar to the tool wear, after each cutting pass, R_a was evaluated. R_a was measured in two axial regions (begin and end of workpieces) and three equally radial directions. Thus, R_a values presented in this paper are the arithmetic average of these six roughness measurements.

Therefore, the responses were the cutting efforts in high-speed turning using a dry and cold air system, with new and worn cutting tools. A piezoelectric dynamometer was used to measure the cutting force (F_c), feed force (F_f), and passive force (F_p). The signal was captured using a four-channel dynamometer model 9272 connected to a signal amplifier model 5070A and set up with a sample rate of 500 Hz. Figure 4b shows the setup used in experimental cutting force tests. Table 4 shows the order in which the experiments were carried out and the condition in which each cutting tool was used, i.e., its flank wear (VB_{max}) values.

According to the tests order shown in Table 4 and the setup exhibited in Fig. 4, each experiment was performed with 8 mm in the longitudinal length of the workpiece with depth of cut (a_p) and feed rate (f) constant equal to 0.8 mm and 0.2 mm/rev, respectively. The influence of the input variables and their interactions on the responses of cutting force (F_c), feed force (F_f), and passive force (F_p) were verified using the analysis of variance (ANOVA) with a significance level of 5% (P value). Thus, it was possible to analyse and obtain the variation of the cutting efforts in the turning with high cutting speeds for new and worn cutting tools.

3 Analysis and discussion of results

3.1 Wear of cutting tools

Figure 5 shows the progress of flank wear (VB_{max}) of TNMG 160408-MF (GC 1125) cutting tool in turning of the API 5L X70 steel. The turning tests represented in Fig. 6 were carried out using the dry condition and cold air system, with cutting speed of 200 m/min, feed rate of 0.2 mm/rev, and depth of cut of 0.8 mm.

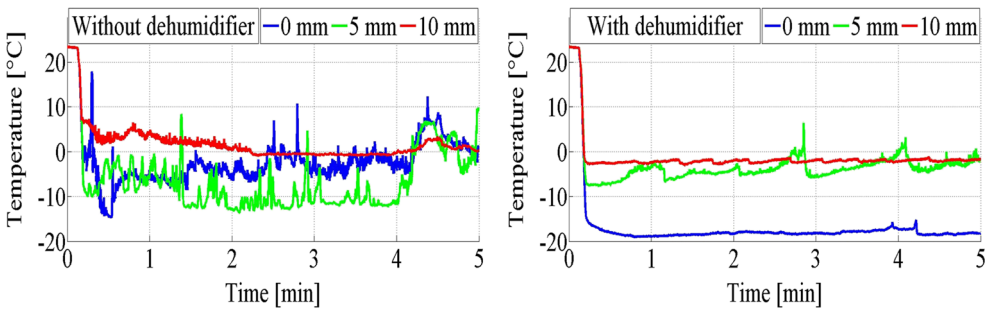

Fig. 3 Monitoring cold air system—room temperature of 23 °C and air pressure in the vortex tube inlet of 5.4 bars

Table 3 Cutting parameters used in high-speed turning

Order of the experiments	Machining condition	Cutting speed (m/min)	Depth of cut (mm)	Feed rate (mm/rev)
1	Dry	200	0.8	0.2
2		400		
3		600		
4	Air cold	200	0.8	0.2
5		400		
6		600		

According to Fig. 5, the progress of tool wear in dry turning with cutting speed of 200 m/min was conducted in six different cutting passes. These cutting passes occurred as follows: the first three cutting passes performed a total machined length of 10,023.0 m, initiating the formation of a small notch in the clearance surface of the cutting tool, which reached a VB_{max} of 0.045 mm at the end of the third cutting pass. In these conditions, a slight abrasive wear on the tip of the cutting tool could also be verified.

During the fourth and fifth cutting passes, an acceleration in the notch wear occurred in the clearance surface of the cutting tool. Furthermore, at the end of these cutting passes, the adhesion of the workpiece material to the cutting tool as well as the start of crater wear formation were verified. At the end of the fifth cutting pass, the machined cutting length was 19,605.3 m and the notch wear on the clearance surface of the cutting tool reached a VB_{max} of 0.148 mm.

Considering the cutting speed of 200 m/min, the dominant type of wear generated in the cutting tools was the notch formation on the clearance surfaces. According to Fig. 5, the cold air system allowed a machined cutting length greater than dry turning. The use of a cold air system increased machining by 4469.37 m more than dry turning. This also corresponds to a 21.8% increase in tool life.

Moreover, the evolution of flank wear (VB_{max}) in experiments with the cold air system was slower than experiments carried out with a dry condition. It can be considered that the decrease in temperature, generated by the cold air system, has favoured the increase in tool life and contained the progress of wear. Temperature is the one greatly responsible for tool wear. Usually, the diffusion mechanism is accelerated with the increase in temperature because it provides energy strong enough to overcome energy barriers of the atomic motion. Based on this, it can be supported that the cold air system was very efficient, because it was capable of maintaining a thermal balance in the cutting region and did not allow a quick increase in temperature, avoiding an acceleration of the diffusion mechanism.

According to Shaw [7], notch wear formation on the clearance surface of the cutting tool has occurred due to the attrition between this surface and the workpiece. Furthermore, the presence of this notch wear has weakened the tip of the cutting tool, since after the sixth cutting pass, i.e. when the total machined cutting length was increased to 20,501.5 m, the cutting tool failed and its tip chipped reaching a VB_{max} of 1.071 mm. Aslantas et al. [16] affirm that the crater wear is the dominant wear type in both uncoated and coated cutting tools. However, coated cutting tools are more inclined to build up edge formation because the TiN coating has approximately tripled both wear resistances.

Moreover, as noted by Settineri et al. [22] in carbide tools (ISO K20 94 wt% WC-6 wt% Co), the coefficient of friction of the substrate is greater than the coating of coated tools. Thus, with the degradation of the coating due to the crater formation in the rake surface, the workpiece material comes

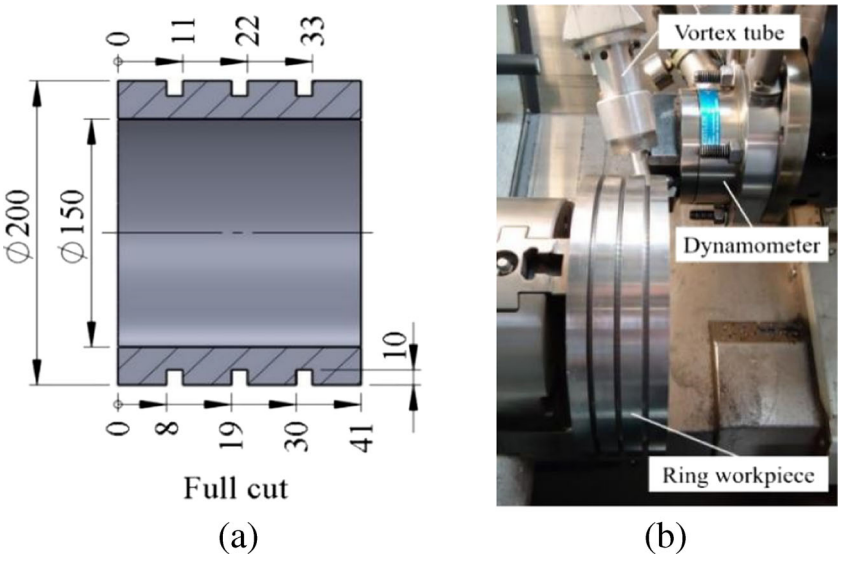

Fig. 4 **a** Layout of the workpiece (dimensions in millimetres). **b** Detail of cutting force experiments

Table 4 Cutting parameters used in high-speed turning to measure cutting forces

Tests order	VB_{max} (mm)	Cutting condition	Cutting speed (m/min)
1	0.000	Cold air	600
2	0.488	Cold air	600
3	0.000	Cold air	400
4	0.581	Cold air	400
5	0.000	Cold air	200
6	1.207	Cold air	200
7	0.000	Dry	600
8	0.481	Dry	600
9	0.000	Dry	400
10	0.772	Dry	400
11	0.000	Dry	200
12	1.071	Dry	200

into direct contact with the substrate of the cutting tool, and due to this high friction coefficient of the substrate, it undergoes the action of the adhesion wear mechanism.

Figure 6 shows the cutting tool with VB_{max} = 1.071 mm; it was used in dry turning with cutting speed of 200 m/min. Figure 6a–d shows, respectively, the SEM of the worn region, the clearance surface, the tip, and the rake surface of the cutting tool.

Figure 7 shows a SEM of the cutting tool used in dry turning with cutting speed of 200 m/min, obtained by SE mode (secondary electrons) with 15 kV of voltage accelerating.

Figure 7 shows in detail the region "A" where the EDS analysis was performed. EDS analysis on a rough surface (low polishing) can greatly increase the error of quantification of the spectrum obtained. Thus, the spectrum EDS obtained for the cutting tools used in this paper will be used only for qualitative identification of the chemical composition of the cutting tool surfaces.

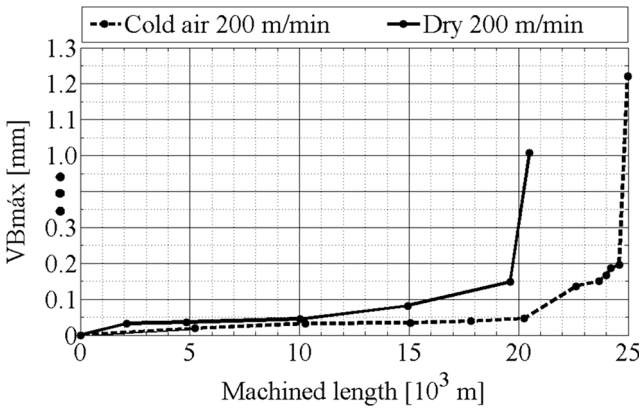

Fig. 5 Flank wear progress of TNMG 160408-MF (GC 1125) with cutting speed of 200 m/min, feed rate of 0.2 mm/rev, and depth of cut of 0.8 mm

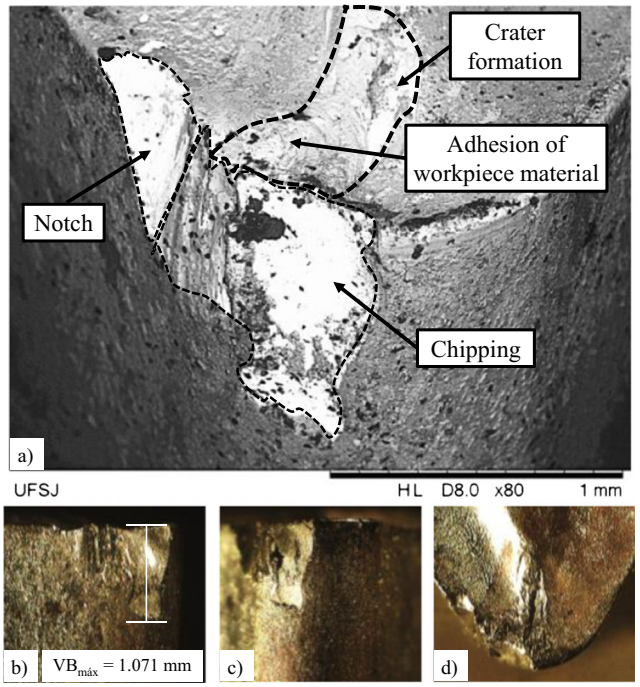

Fig. 6 Cutting tool with VB_{max} = 1.071 mm used in dry turning with cutting speed of 200 m/min. **a** SEM. **b** Clearance surface. **c** Tip. **d** Rake surface

Figure 8 shows the spectrum EDS analysis performed in region A of the cutting tool shown in Fig. 7. Thus, the presence of the chemical elements carbon (C), chrome (Cr), iron (Fe), cobalt (Co), and tungsten (W) can be verified. Relating Figs. 7 and 8, it was verified that the chemical element Fe was found in the darker area of region A, which characterizes the adhesion of the workpiece material to the rake surface of the cutting tool. On the other hand, the chemical elements C, Cr, Co, and W were found in the lighter area of region A, characterizing the substrate of the cutting tool (carbide tool). In the lighter area of region A, some scratches caused by attrition can

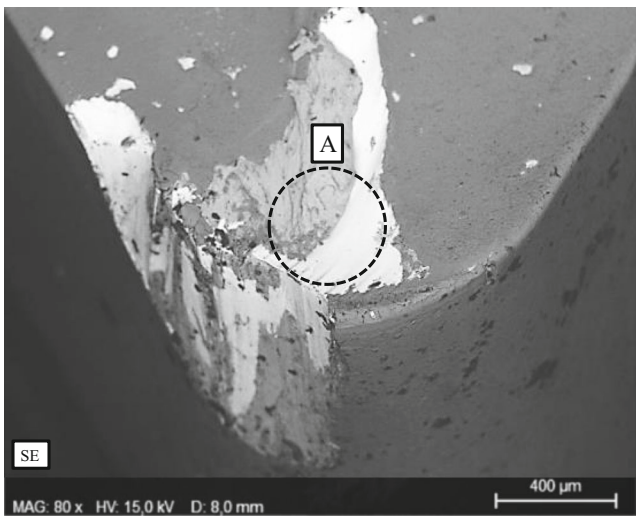

Fig. 7 EDS of cutting tool used in dry turning with cutting speed of 200 m/min, obtained by SE mode

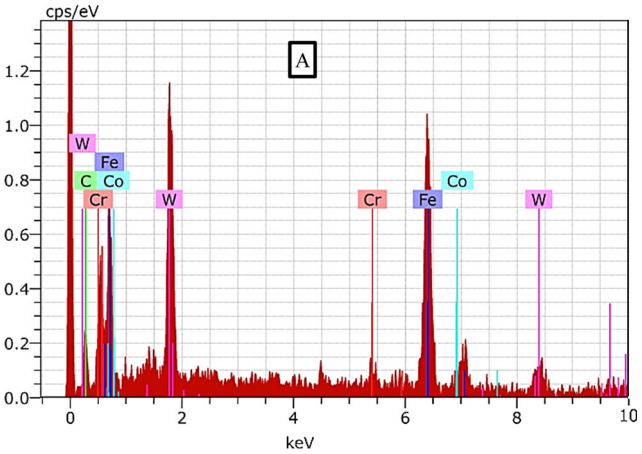

Fig. 8 Spectrum EDS analysis performed in region "A" of the cutting tool used in dry turning with cutting speed of 200 m/min

be seen, a result of the sliding of the chip on the rake surface of the cutting tool, and also a region with a smooth appearance is perceived, suggesting the action of an adhesion mechanism.

Thus, it can be concluded that the type of wear verified in the cutting tool used in dry turning with cutting speed of 200 m/min, feed rate of 0.2 mm/rev, and depth of cut of 0.8 mm was the formation of a notch and crater, with abrupt failure (chipping), through the action of adhesion wear mechanism and, mainly, attrition.

Returning to the analysis of Fig. 5, it can be verified that the progress of tool wear in turning with the cold air system and cutting speed of 200 m/min occurred in 11 different cutting passes. These cutting passes can be described as follows: the first three cutting passes generated a machined cutting length of 15,054.80 m and induced a small flank wear (VB_{max}) of 0.034 mm. Furthermore, the formation of a notch at the end of the clearance surface of the cutting tool can be verified, after the third cutting pass. Besides, at the end of the third cutting pass, a slight abrasive wear on the tip of the cutting tool and some risks on the rake surface caused by the sliding of the chip could also be verified.

In the fourth and fifth cutting passes, the machined cutting length increased to 20,256.6 m, and the notch in the clearance surface of the cutting tool slightly increased and reached a VB_{max} of 0.046 mm. The rake surface of the cutting tool presented no change, except for a slight wear on the tip of the cutting tool that was more significant, which suggests a gradual loss of the cutting tool coating.

After the sixth and seventh cutting passes, the machined cutting length was increased to 23,666.60 m. During the performance of these cutting passes, an acceleration of the notch wear on the clearance surface of the cutting tool can be verified, reaching a VB_{max} of 0.150 mm, at the end of the seventh cutting pass, as can be seen in Fig. 9. It can be considered that the cooling of the cutting zone, generated by the cold air system, has contained, a little, the increase of notch wear compared to dry turning. This might have happened because, for the same notch wear, i.e., VB_{max} of 0.148 mm for the dry turning, VB_{max} was 0.150 mm for the turning with the cold air system. Thus, the use of the cold air system allowed an increase in the machining length of 4061 m, and this length represented a gain of 20.7% in tool life.

However, the presence of notch wear on the clearance surface in the cooling may have changed the geometry of the cutting tool and, therefore, the formation of the chips, because the chips that initially showed a small helical shape (about 5–7 cm of length) began to present a continuous format. Thus, due to the small distance between the nozzle and the vortex tube, the continuous chips began to accumulate between the cutting tool and the output of cold air (Fig. 9c). Therefore, seeking to avoid the chip accumulation, the next cutting passes were performed with a reduced machined length.

By reducing the machined cutting length, the accumulation of chip between the cutting tool and the cold air output was avoided. However, it can be considered that the continuous formation of chips accelerated the notch wear in the clearance surface weakening the cutting tool. Based on this, after the 11th cutting pass, when the total cutting length reached 24,970.80 m, the cutting tool failed abruptly and its tip chipped, generating a VB_{max} of 1.207 mm.

Figure 10 shows the cutting tool with VB_{max} of 1.207 mm. In this experiment, the cold air system and a cutting speed of 200 m/min was used. Figure 10a–d shows, respectively, the SEM of the worn region, the clearance surface, the tip, and the rake surface of the cutting tool. Figure 11 shows the SEM obtained by SE mode (secondary electrons) with 15 kV accelerating voltage and region A where the EDS analysis was performed.

Figure 12 shows the spectrum EDS analysis performed in region A. The presence of chemical elements carbon (C), chrome (Cr), iron (Fe), cobalt (Co), and tungsten (W) can be verified. Regarding Figs. 11 and 12, the chemical element Fe was found in the darkest area of region A, characterizing the adhesion of the machined material on the cutting tool tip. On the other hand, the chemical elements C, Cr, Co, and W were found in the clearest area of region A, characterizing the substrate of the cutting tool.

As previously mentioned, according to Settineri et al. [22], the cutting tool substrate has a coefficient of friction greater than the coating coefficient of friction. Thus, the chipping of the tip of the cutting tool put the substrate directly in contact with the machined material. Thus, due to the high friction coefficient of the substrate, the adhesion wear mechanism began to be effective.

Thus, it can be concluded that the type of wear verified in the cutting tool with the cold air system and cutting speed of 200 m/min, feed rate of 0.2 mm/rev, and depth of cut of 0.8 mm was the formation of a notch, with abrupt failure (chipping), due to the increase of attrition and the adhesion

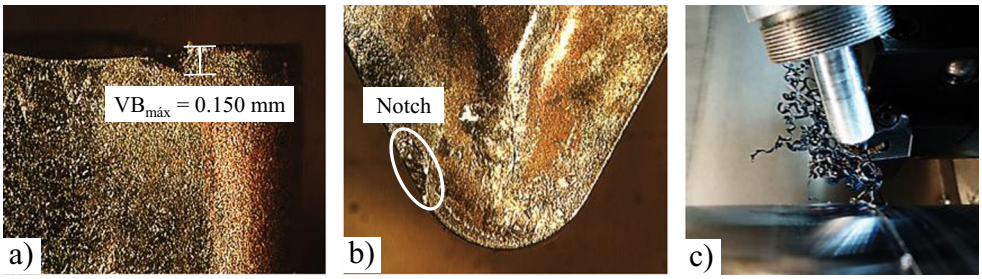

Fig. 9 Cutting tool used in turning with cold air system, with cutting speed of 200 m/min

wear mechanism. Therefore, it can be defined that the cold air system showed satisfactory results when compared to dry turning, because it allowed the machining of a cutting length higher than dry turning.

Figure 13 shows the progress of flank wear (VB_{max}) of TNMG 160408-MF (GC 1125) cutting tool during the machining of API 5L X70 steel. The turning tests represented by Fig. 13 were carried out with dry and cold air conditions, with cutting speed of 400 m/min, feed rate of 0.2 mm/rev, and depth of cut of 0.8 mm.

All VB_{max} values shown in Fig. 13 were measured on the tips of the cutting tools. For the cutting speed of 400 m/min, the main kind of wear was the attrition. According to Fig. 13, the cold air system allowed a machined cutting length greater than dry turning. The use of the cold air system increased the machining by 58.5 m more than the dry turning, which corresponds to an increase by 5.2% in tool life.

Also in experiments performed with cutting speed of 200 m/min, in experiments with cutting speed of 400 m/min and with cold air system, the evolution of flank wear (VB_{max}) was slower than in experiments carried out with dry air. It is believed that the decrease in temperature in the cutting zone generated by the cold air system contributed with the increase of tool life and avoided a part of the wear progress.

Comparing the experiments carried out with cutting speeds of 200 and 400 m/min, it can be seen that the increase in cutting speed had a great influence in the tool life. In dry condition, the increase in the cutting speed from 200 to 400 m/min reduced the machined cutting length by 21 times, whereas when the cold air system was used the reduction in machined cutting length was by 18 times. According to Shaw [7], the increase in cutting speed promotes the increase in cutting temperature, resulting directly in increase of tool wear and therefore in tool life.

According to Fig. 13, the progress of tool wear in dry turning with cutting speed of 400 m/min was performed only in two cutting passes. The process was carried out as follows: in the first cutting pass, the machined cutting length was 888.9 m and the cutting tool showed a high abrasive wear in its tip reaching a VB_{max} of 0.180 mm. Moreover, abrasive scratches could also be seen in the rake surface of the cutting tool, indicating the tendency to crater formation. After the second cutting pass, the machined cutting length increased to 1133.0 m and the cutting tool showed a high abrasive wear

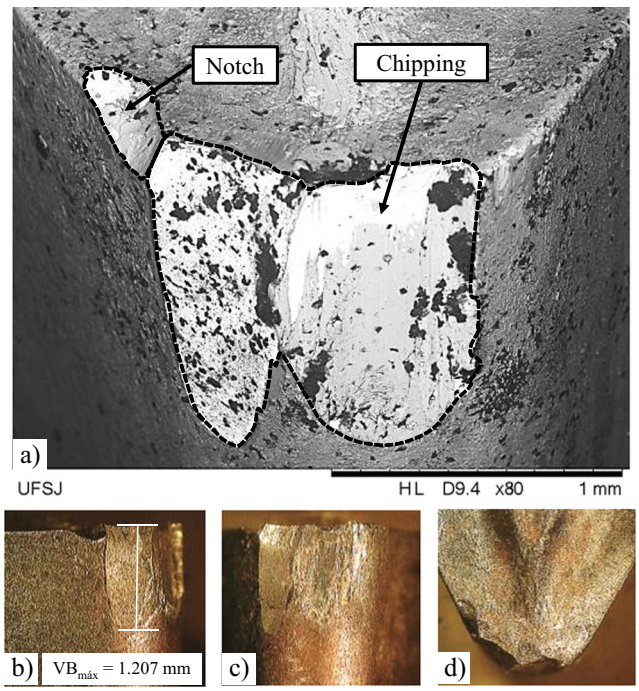

Fig. 10 Cutting tool with VB_{max} = 1.207 mm used in turning with the cold air system with cutting speed of 200 m/min. **a** SEM. **b** Clearance surface. **c** Tip. **d** Rake surface

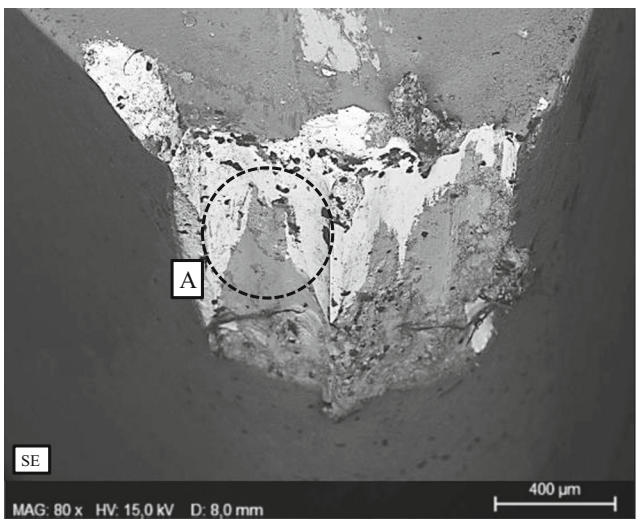

Fig. 11 EDS of cutting tool used in turning with the cold air system with cutting speed of 200 m/min, obtained by SE mode

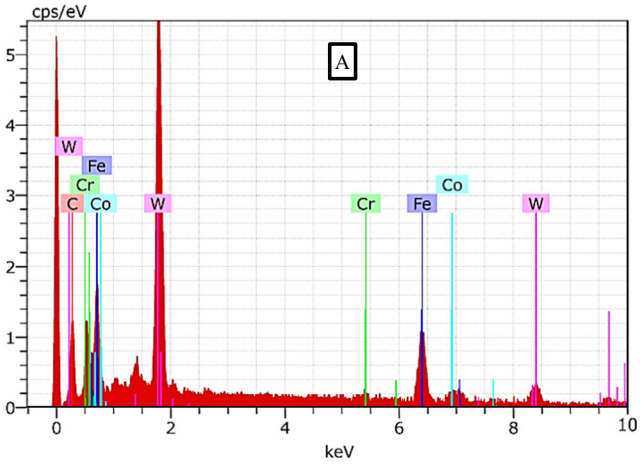

Fig. 12 Spectrum EDS analysis performed in region "A" of the cutting tool used in turning with the cold air system with cutting speed of 200 m/min

in its tip, reaching a VB_{max} of 0.772 mm, which was defined as its end of life. Furthermore, after this cutting pass, the crater formation in the rake surface of the cutting tool was confirmed.

Figure 14 shows the cutting tool with VB_{max} of 0.772 mm after the dry turning with cutting speed of 400 m/min. Figure 14a–d shows, respectively, the SEM of the worn region, the clearance surface, the tip, and the rake surface of the cutting tool. Figure 15 shows a SEM of the cutting tool used in dry turning with cutting speed of 400 m/min, obtained by SE mode (secondary electrons) with 15 kV accelerating voltage. Regions A and B can be seen where the EDS analysis were performed.

Figure 16 shows the spectrum EDS analysis performed in regions A and B of the cutting tool shown in Fig. 15. Thus, the presence of chemical elements carbon (C), chrome (Cr), iron (Fe), cobalt (Co), and tungsten (W) in region "A" and only carbon (C) and tungsten (W) in region "B" can be verified. In relation to Figs. 15 and 16, the chemical element Fe was found

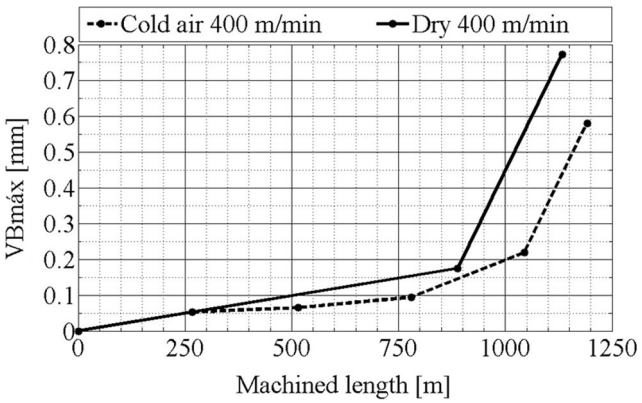

Fig. 13 Flank wear progress of TNMG 160408-MF (GC 1125) with cutting speed of 400 m/min, feed rate of 0.2 mm/rev, and depth of cut of 0.8 mm

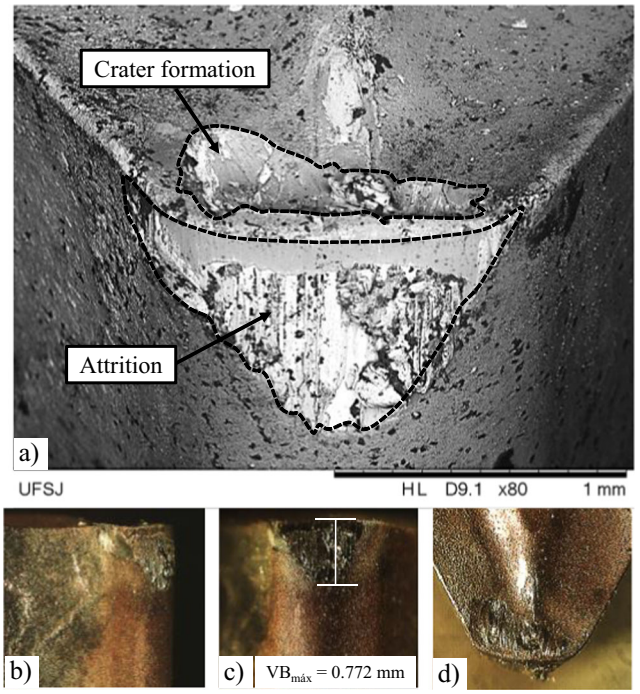

Fig. 14 Cutting tool with VB_{max} = 0.772 mm used in dry turning with cutting speed of 400 m/min. **a** SEM. **b** Clearance surface. **c** Tip. **d** Rake surface

in the darkest area of region A, characterizing the adhesion of machined material to the rake surface of the cutting tool.

On the other hand, the chemical elements C, Cr, Co, and W were found in the clearest area of region A, characterizing the substrate of the cutting tool. Across region B, only the chemical elements C and W were found, also characterizing the substrate of the cutting tool. The clearest area of region A presents a smooth appearance, which suggests that the crater formation occurs by the action of the adhesion mechanism. In region B, scratches caused by the attrition between the machined material and the cutting tool can be seen.

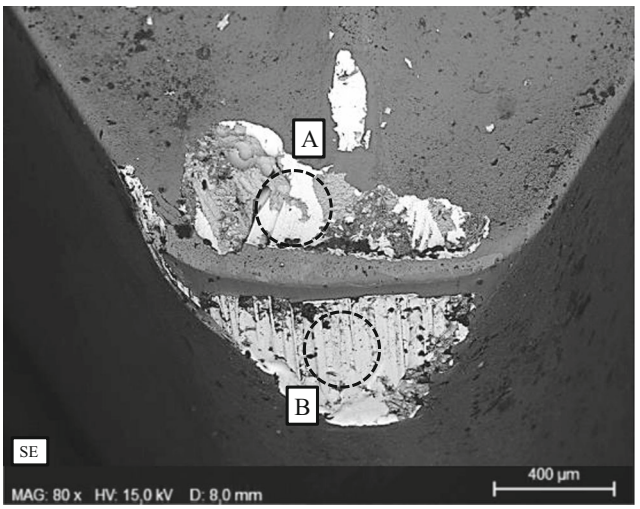

Fig. 15 EDS of the cutting tool used in dry turning with cutting speed of 400 m/min, obtained by SE mode

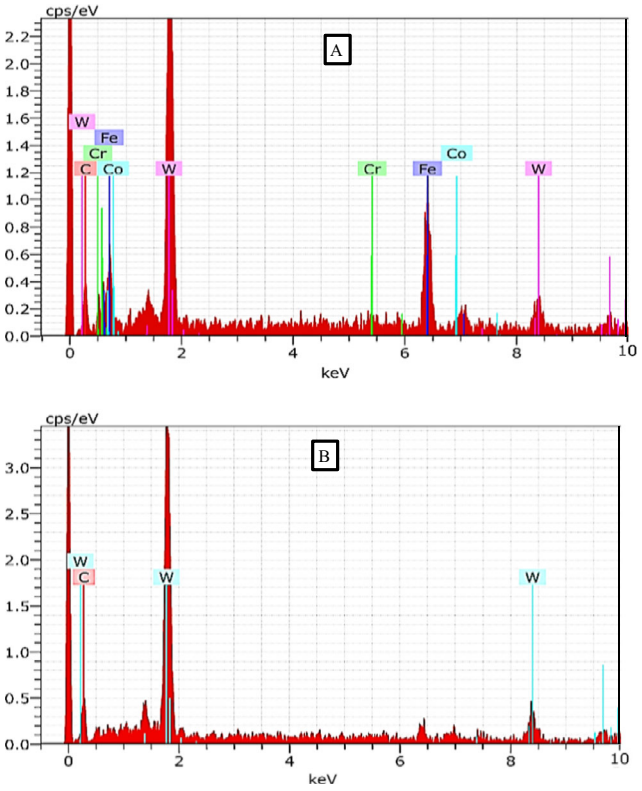

Fig. 16 Spectrum EDS analysis performed in regions "A" and "B" of the cutting tool used in dry turning with cutting speed of 400 m/min

Thus, it can be concluded that the types of wear verified in the cutting tool used in dry turning with cutting speed of 400 m/min, feed rate of 0.2 mm/rev, and depth of cut of 0.8 mm were the flank wear and the crater wear, through the action of adhesion wear mechanism and, mainly, by the attrition. Returning to Fig. 13, it can be verified that the progress of the tool wear in turning with the cold air system and cutting speed of 400 m/min was carried out in five different cutting passes. This process was performed as follows: the first two cutting passes generated a machined cutting length of 515.8 m, and a small abrasive wear in the tip of the cutting tool (VB_{max}) equal to 0.065 mm occurred. Slight abrasive scratches could also be verified in the rake surface, which were caused by the sliding of the chip.

After the third cutting pass, the machined cutting length was increased to 780.1 m and the flank wear (VB_{max}) reached 0.095 mm. Moreover, adhesion of the machined material in the rake surface of the cutting tool could also be verified. It is believed that the cold air system has promoted the reduction of the temperature at the cutting zone. This decrease in temperature provided a cooling in the chips, which increased their attrition resistance on the rake surface, thus allowing the adhesion of the machined material to the rake surface of the cutting tool.

After the fourth cutting pass, the machined cutting length was increased to 1044.0 m, and the flank wear reached a VB_{max} of 0.220 mm. It can be noticed that the adhesion of the machined material enhanced, and the beginning of crater formation also occurred in the rake surface. Finally, after the fifth cutting pass, the total machined cutting length was 1191.0 m and the wear reached a VB_{max} of 0.581 mm determining the end of tool life. Moreover, there was adhesion of the machined material to the worn region of the tool tip and to the rake surface as well as the formation of a crater in the rake surface.

Figure 17 shows the cutting tool with VB_{max} of 0.581 mm with the cold air system and cutting speed of 400 m/min. Figure 17a–d shows, respectively, the SEM of the worn region, the clearance surface, the tip, and the rake surface of the cutting tool. Figure 18 shows a SEM of the cutting tool used in turning with the cold air system, with cutting speed of 400 m/min, obtained by SE mode (secondary electrons) with 15 kV accelerating voltage. Thus, regions A and B can be seen where the EDS analysis was performed.

Figure 19 shows the spectrum EDS analysis performed in regions A and B of the cutting tool shown in Fig. 18. Thus, the presence of chemical elements carbon (C), iron (Fe), cobalt (Co), and tungsten (W) can be verified in both regions A and B. However, in region A the presence of chrome (Cr) can also be verified. Relating Figs. 18 and 19, the chemical element Fe was found in the darkest areas of regions A and B characterizing the adhesion of the machined material to the rake surface and to the tip of the cutting tool.

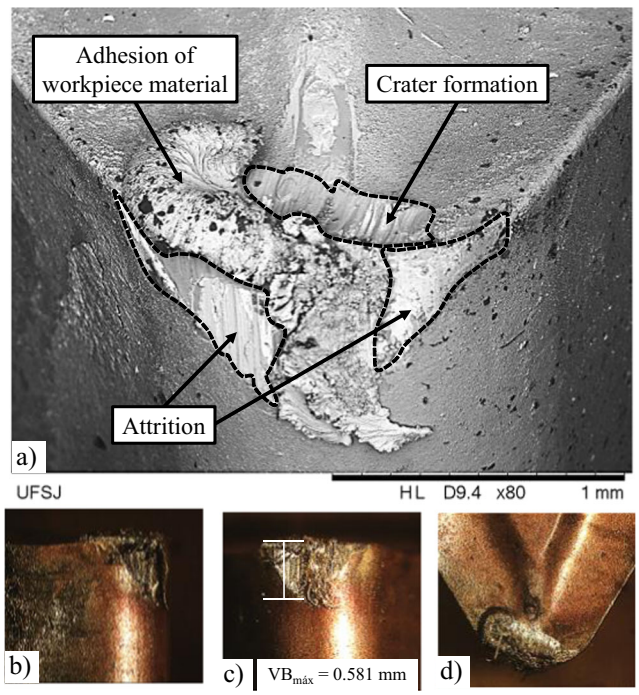

Fig. 17 Cutting tool with VB_{max} = 0.581 mm used in turning with the cold air system, with cutting speed of 400 m/min. **a** SEM. **b** Clearance surface. **c** Tip. **d** Rake surface

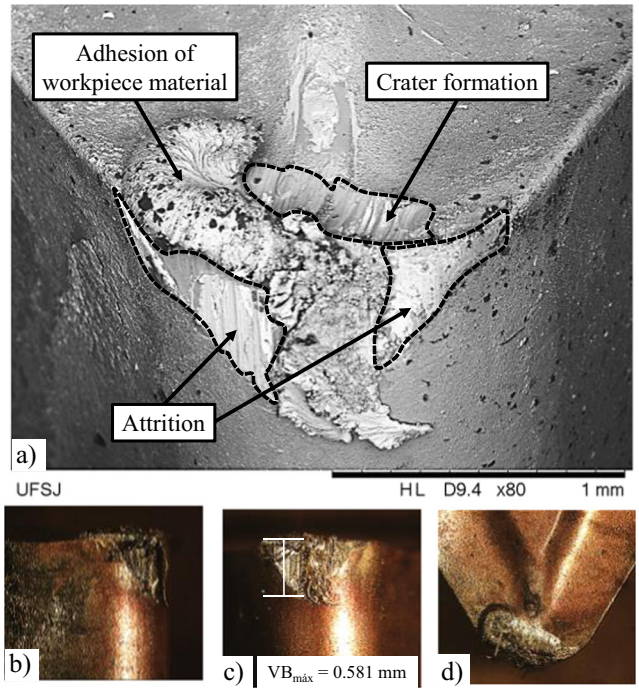

Fig. 18 EDS of cutting tool used in turning with the cold air system, with cutting speed of 400 m/min, obtained by SE mode

On the other hand, the chemical elements C, Co, and W were found in the clearest areas of regions A and B, which shows the substrate of the cutting tool. The chemical element Cr was also found in the clearest area of region A and in a part of the substrate of the cutting tool. In both regions A and B, more scratches caused by attrition between the machined material and the cutting tool can be seen.

Thus, it can be concluded that the types of wear verified in the cutting tool used in turning with the cold air system with cutting speed of 400 m/min, feed rate of 0.2 mm/rev, and depth of cut of 0.8 mm were the flank wear and the crater wear, through the action of the adhesion wear mechanism and, mainly, by attrition. Figure 20 shows the progress of flank wear (VB_{max}) of TNMG 160408-MF (GC 1125) during the turning process of the API 5L X70 steel. The turning tests represented by Fig. 20 were carried out to dry using a cold air system, with cutting speed of 600 m/min, feed rate of 0.2 mm/rev, and depth of cut of 0.8 mm.

All VB_{max} values shown in Fig. 20 were measured in the tips of the cutting tools and for the cutting speed of 600 m/min. The main type of wear in the cutting tools was the attrition in their tips. According to Fig. 20, the cold air system allowed a machined cutting length greater than dry turning. The use of a cold air system increased machining by 58.0 m more than dry turning. This also corresponds to a 31.7% increase in tool life. As well as in experiments performed with cutting speeds of 200 and 400 m/min, in experiments with cutting speed of 600 m/min and with a cold air system, the evolution of the flank wear (VB_{max}) was slower than experiments carried out with the dry system. It is believed that the decrease in the cutting zone temperature, generated by the cold air system, has favoured the increase in the tool life, decreasing the tool wear.

Comparing the experiments carried out with cutting speeds of 200 and 600 m/min, it can be seen that the increase in the cutting speed had a great influence in tool life. In dry turning, the increase in the cutting speed from 200 to 600 m/min reduced the machined cutting length 111 times, whereas in turning with the cold air system the reduction in machined cutting

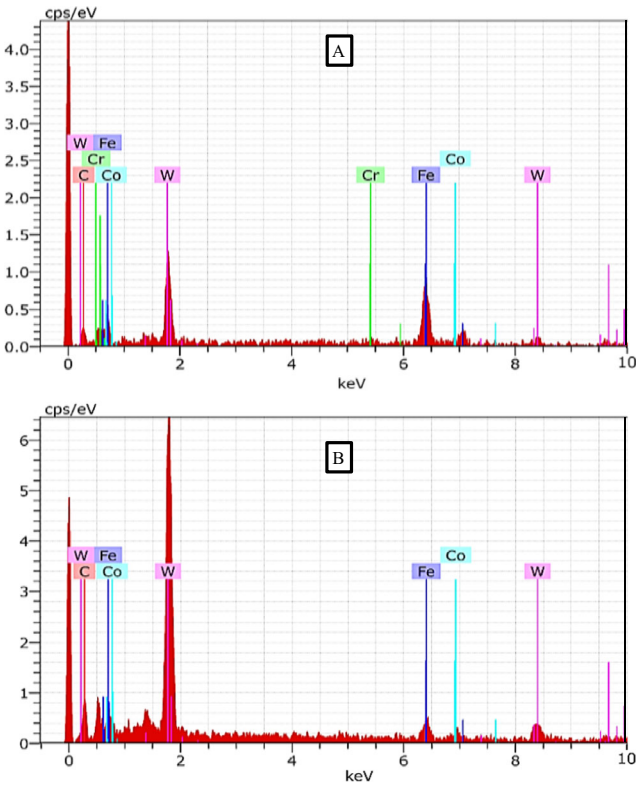

Fig. 19 Spectrum EDS analysis performed in regions "A" and "B" of the cutting tool used in turning with cold air system, with cutting speed of 400 m/min

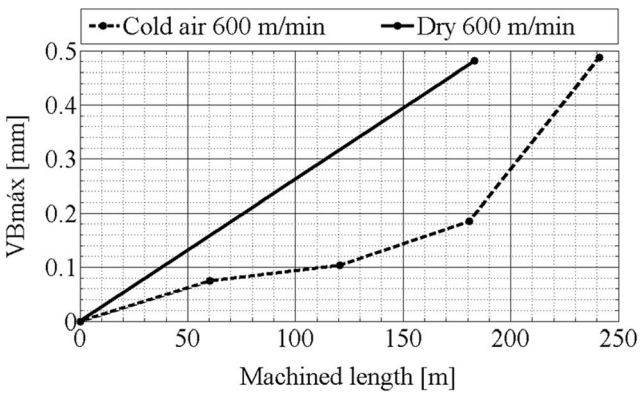

Fig. 20 Flank wear progress of TNMG 160408-MF (GC 1125) with cutting speed of 600 m/min, feed rate of 0.2 mm/rev, and depth of cut of 0.8 mm

length was 103 times. As previously mentioned, it can be seen that the assertion of Shaw [7] is found and the increase in cutting speed promotes the increase in cutting temperature, acting directly in the reduction of tool life.

According to Fig. 20, the tool wear in dry turning with cutting speed of 600 m/min was performed with just one cutting pass. This was carried out as follows: in this cutting pass, the machined cutting length was 183.2 m and the cutting tool reached its end of life. Thus, the cutting tool showed a high abrasive wear on its tip with a VB_{max} of 0.481 mm. Moreover, crater formation can also be seen in the rake surface of the cutting tool. Figure 21 shows the cutting tool with VB_{max} of 0.481 mm with cutting speed of 600 m/min. Figure 21a–d shows, respectively, the SEM of the worn region, the clearance surface, the tip, and the rake surface of the cutting tool.

Figure 22 shows a SEM of the cutting tool used in dry turning with cutting speed of 600 m/min, obtained by SE mode (secondary electrons) with 15 kV accelerating voltage. Thus, region A, where the EDS analysis was performed, can be seen.

Figure 23 shows the spectrum EDS analysis performed in region A of the cutting tool shown in Fig. 22. Thus, the presence of chemical elements carbon (C), chrome (Cr), iron (Fe), cobalt (Co), and tungsten (W) can be verified in this region. Relating Figs. 22 and 23, the chemical element Fe was found in the darkest area of region A, characterizing the adhesion of the machined material to the rake surface of the cutting tool. On the other hand, the chemical elements C, Cr, Co, and W were found in the clearest area of region A, characterizing the

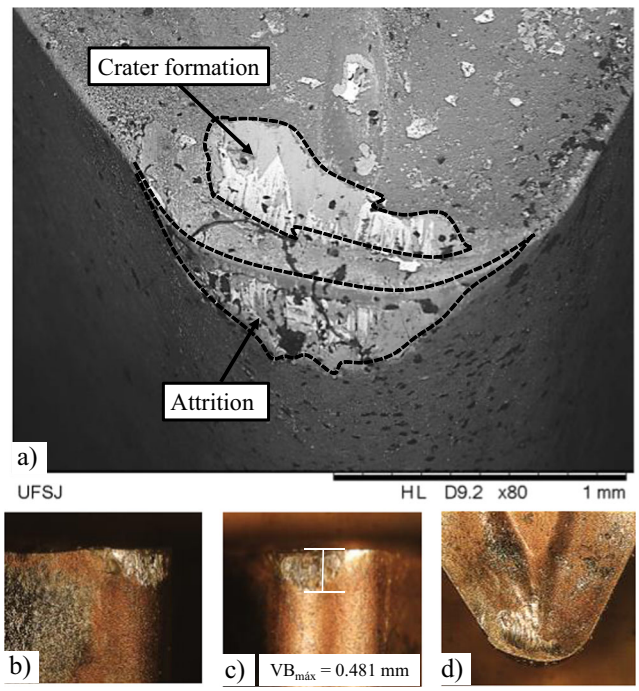

Fig. 21 Cutting tool with VB_{max} = 0.481 mm used in dry turning with cutting speed of 600 m/min. **a** SEM. **b** Clearance surface. **c** Tip. **d** Rake surface

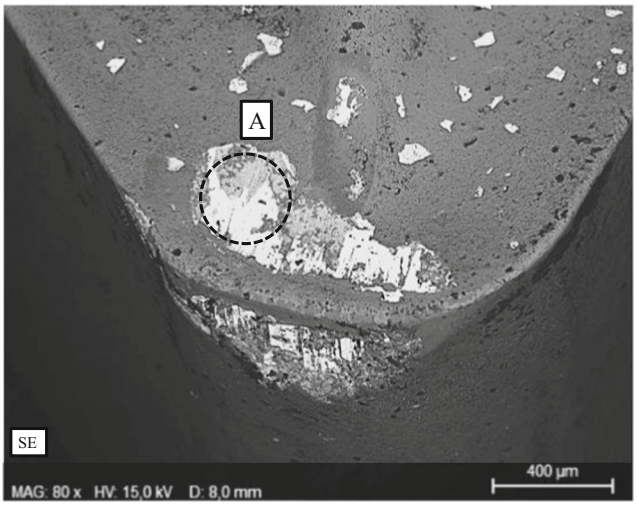

Fig. 22 EDS of cutting tool used in dry turning with cutting speed of 600 m/min, obtained by SE mode

substrate of the cutting tool. Both in the rake surface and in the tip of the cutting tool, scratches caused by attrition between the machined material and the cutting tool can be seen.

Thus, it can be concluded that the types of wear verified in the cutting tool used in dry turning with cutting speed of 600 m/min, feed rate of 0.2 mm/rev, and depth of cut of 0.8 mm were the flank wear and the crater, through the action of attrition wear mechanism. Returning to Fig. 20, it can be also verified that the tool wear with a cold air system and cutting speed of 600 m/min was evaluated in four equal cutting passes. This process was carried out as follows: the first three cutting passes reached a machined cutting length of 180.9 m and generated an abrasive wear in the tip of the cutting tool with VB_{max} of 0.185 mm.

After the fourth cutting pass, the machined cutting length increased to 241.2 m and the abrasive wear in the tip of the cutting tool was a dominant phenomenon and reached a VB_{max} of 0.488 mm when the end of tool life was determined. Moreover, after this cutting pass, the beginning of crater formation in the rake surface of the cutting tool can also be seen. Although the cold air system has allowed a slower progress of the flank wear than in the dry turning, it is believed that the use of the high cutting speed of 600 m/min has promoted an increase of temperature in the cutting zone. Therefore, there was no action of the adhesion wear mechanism, as seen in experiments with cutting speed of 400 m/min. Figure 24 shows the cutting tool with VB_{max} = 0.581 mm; it was used in turning with the cold air system with cutting speed of 400 m/min. Figure 24a–d shows, respectively, the SEM of the worn region, the clearance surface, the tip, and the rake surface of the cutting tool.

Thus, it can be concluded that the types of wear verified in the cutting tool used in turning with the cold air system, cutting speed of 600 m/min, feed rate of 0.2 mm/rev, and depth of cut of 0.8 mm were the flank wear and the crater, through the

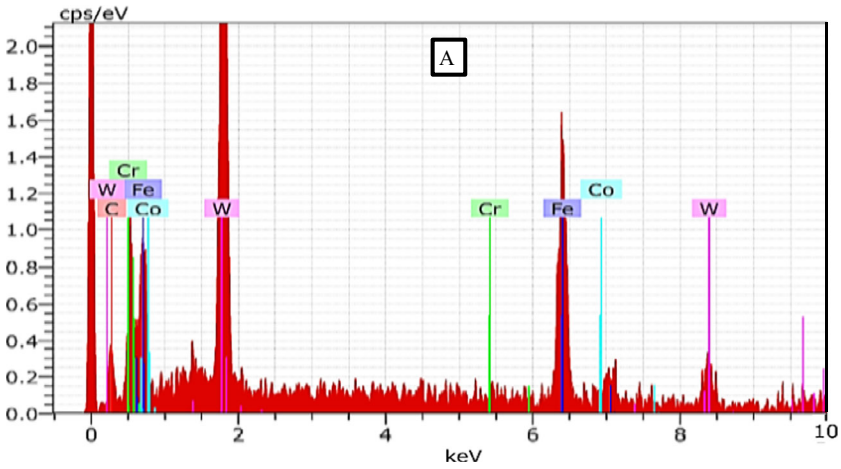

Fig. 23 Spectrum EDS analysis performed in region "A" of the cutting tool used in dry turning with cutting speed of 600 m/min

action of the attrition wear mechanism. After the fourth experiment, one more test was performed that generated the catastrophic failure of the tool. Thus, the EDS analysis was not performed because the tool tip was fractured, as can be seen in Fig. 25.

3.2 Analysis of cutting efforts

Figure 26 shows a typical behaviour of the cutting efforts resulting from the turning experiments of this work. To perform the analysis of variance, the values of the cutting efforts were obtained through the arithmetic averages of three measurements of these efforts, performed at the start point, medium point, and end point for each cut interval. The cut interval is understood as the time interval in which the cutting tool effectively performs the cutting of the material. In Fig. 26, for instance, the cut interval ranged approximately between 1.0 and 4.0 s.

Figure 27 shows the variation of the cutting efforts in high-speed turning of API 5L X70 steel using a dry and cold air system, new cutting tools TNMG 160408-MF (GC 1125) (VB_{max} = 0 mm), feed rate of 0.2 mm/rev, and depth of cut of 0.8 mm.

According to Fig. 27, as expected, the cutting force represents the largest share among the cutting efforts, followed by the feed force and the thrust force, respectively. According to Sadik [23] and Chinchanikar and Choudhury [24], when using a depth of cut greater than the tool tip radius, the cutting of the material is performed by both the tool tip radius and the main cutting edge. Thus, it has been found that the feed force is greater than the thrust force. In this study, because the depth of cut is equal to the tool tip radius, it is verified that the feed force and the thrust force present practically the same values.

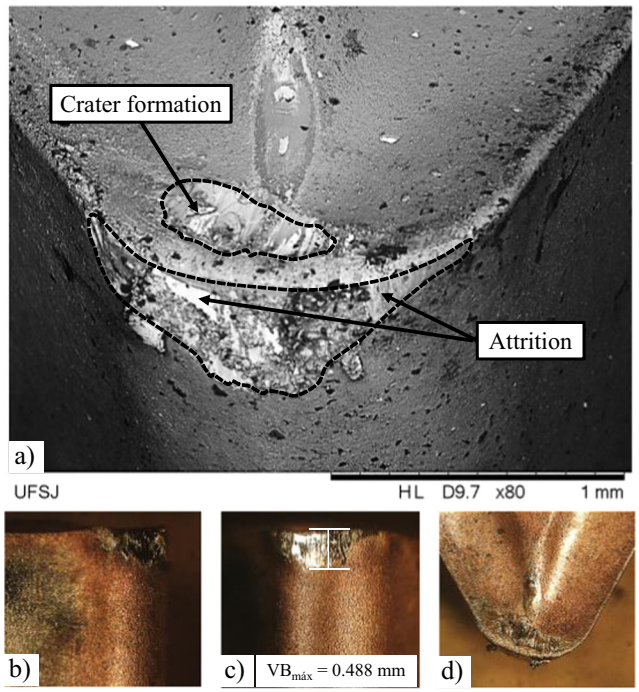

Fig. 24 Cutting tool with VB_{max} = 0.488 mm used in turning with cold air system, with cutting speed of 600 m/min. **a** SEM. **b** Clearance surface. **c** Tip. **d** Rake surface

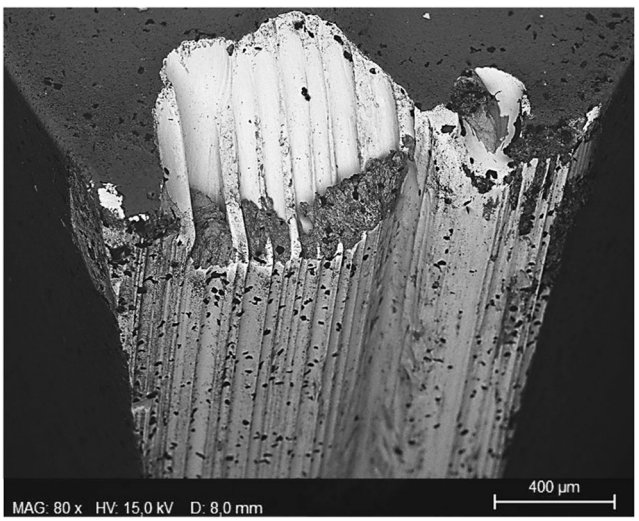

Fig. 25 Cutting tool fractured after the fourth experiment with cutting speed of 600 m/min, feed rate of 0.2 mm/rev, and depth of cut of 0.8 mm

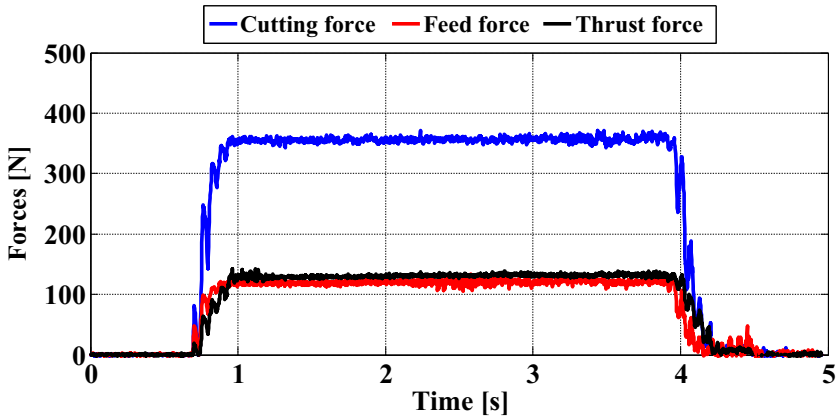

Fig. 26 Cutting forces in turning with a new cutting tool, cold air system, and cutting speed of 600 m/min

Thus, it can be considered in all experiments with new cutting tools (VB_{max} = 0 mm) that the cutting force presented values at least 2.6 times greater than the feed and thrust forces. Moreover, in Fig. 27, a slight reduction in cutting efforts is verified when using the cold air system. Thus, it is believed that the constant flow of cold air, close to the tip of the cutting tool, contributed to the removal of the chips formed, promoting this slight reduction of cutting efforts.

In addition, according to Fig. 27, as expected, the increase in the cutting speed provided a reduction in the cutting efforts, both in dry turning and in turning with the cold air system. It is believed that the reduction of cutting efforts with increasing cutting speed can be explained by the decrease in shear strength of the material. According to Abukhshim et al. [25], Lima et al. [26], Pawade et al. [9, 27], and Khan et al. [28], an increase in cutting speed generates extremely high temperatures in the cutting zone of the material, reducing the shear strength, increasing its plasticity, and, consequently, reducing the cutting efforts.

In turning experiments with the cold air system, the reduction in the cutting force when the cutting speed increased from 200 to 400 m/min was by 7.0% (26.9 N). The increase of the cutting speed from 200 to 600 m/min provided a reduction by 15.1% (53.9 N). In dry turning experiments, the reduction of the cutting force due to the increase of the cutting speed from 200 to 400 m/min was by 5.6% (21.7 N). When the cutting speed increased from 200 to 600 m/min, the reduction was by 13.5% (48.5 N). Thus, the smaller cutting efforts in the turning of API 5L X70 steel, with new cutting tools, were found with a cutting speed of 600 m/min and using the cold air system. The values of the cutting efforts for this condition are cutting force of 356.0 N, feed force of 120.6 N, and thrust force of 131.07 N.

Figure 28 shows the variation of the cutting efforts in the high-speed turning of API 5L X70 steel using the dry and cold air system, worn cutting tools TNMG 160408-MF (GC 1125) (VB_{max} ≥0.3 mm), feed rate of 0.2 mm/rev, and depth of cut of 0.8 mm. The wear condition of each cutting tool is shown in Table 4.

As each cutting tool presented a peculiar flank wear (VB_{max}) and a specific geometry generated by this wear, it is verified, based on Fig. 28, that each cutting condition presented a different behaviour for the cutting efforts. According to Fig. 5, it is verified that the cutting tool used in turning with

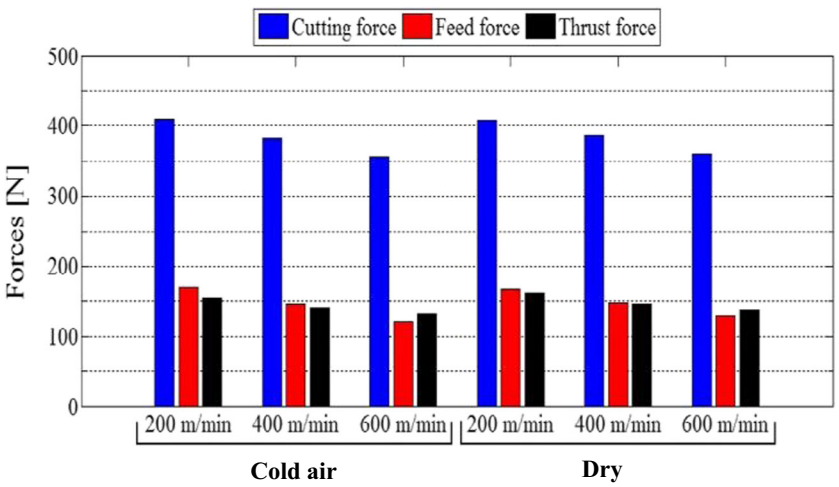

Fig. 27 Cutting forces in turning with new cutting tools TNMG 160408-MF (GC 1125)

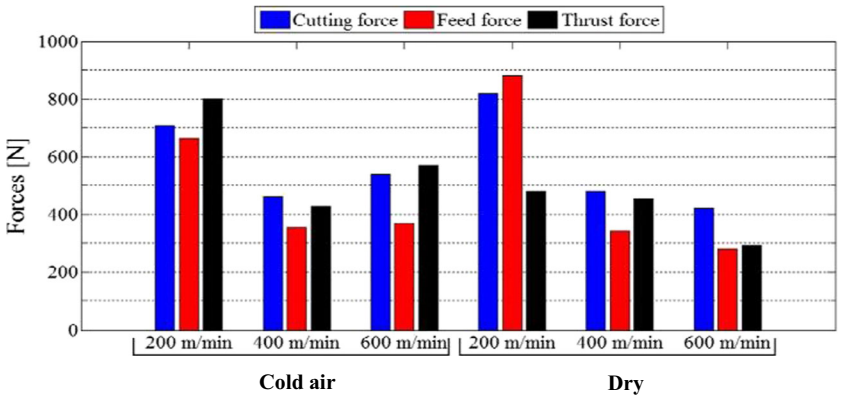

Fig. 28 Cutting forces in turning with worn cutting tools TNMG 160408-MF (GC 1125)

the cold air system with cutting speed of 200 m/min showed a VB_{max} equal to 1.207 mm, generated by the chipping of the tool tip, deriving from the progression of a notch. Thus, according to Figs. 6 and 7, the chipping of the cutting tool tip was responsible for the increase of the cutting efforts and generated a greater friction between the cutting tool and the workpiece, verified by the high increase of feed and thrust forces. If the cutting efforts of the new cutting tool (VB_{max} = 0 mm) are compared with the worn cutting tool (VB_{max} = 1.207 mm), an increase by 73.1% (299.8 N) can be verified in the cutting force, 290.9% (494.4 N) in the feed force, and 420.9% (648.5 N) in the thrust force when using the worn cutting tool.

According to Fig. 13, the cutting tool used in turning with the cold air system with cutting speed of 400 m/min showed a VB_{max} equal to 0.581 mm. This was generated by the attrition between the workpiece and the tip of the cutting tool, in addition to the presence of crater and the adhesion of the material to the workpiece on the rake surface of the tool. Thus, according to Figs. 14 and 15, this wear promoted the increase in the cutting efforts, with the abrasion at the tip of the tool being the major responsible for the generation of a greater friction between the tool and the workpiece, verified by the high increase of the thrust force. If the cutting efforts of the new cutting tool (VB_{max} = 0 mm) are compared with the worn cutting tool (VB_{max} = 0.581 mm), an increase by 21.0% (80.6 N) can be verified in the cutting force, 144.5% (210.7 N) in the feed force, and 203.4% (286.9 N) in the thrust force when using the worn cutting tool.

According to Fig. 20, the cutting tool used in turning with the cold air system, with cutting speed of 600 m/min, showed a VB_{max} equal to 0.488 mm, generated by the attrition between the workpiece and the tip of the cutting tool, besides the presence of a crater on the rake surface of the tool. Thus, according to Figs. 21 and 22, this wear promoted the increase in the cutting efforts, with the abrasion at the tip of the tool being the major responsible for the generation of a greater friction between the tool and the workpiece, verified by the high increase of the thrust force. If the cutting efforts of the new cutting tool (VB_{max} = 0 mm) are compared with the worn cutting tool (VB_{max} = 0.488 mm), an increase by 51.3% (182.7 N) can be verified in the cutting force, 207.8% (250.5 N) in the feed force, and 335.5% (439.8 N) in the thrust force when using the worn cutting tool.

According to Fig. 5, the cutting tool used in dry turning with cutting speed of 200 m/min showed a VB_{max} equal to 1.071 mm, generated by the chipping of the tool tip, coming from the progression of a notch, besides the presence of a crater and the adhesion of the material to the workpiece on the rake surface of the tool. Thus, according to Figs. 6 and 7, the chipping of the cutting tool tip was responsible for the increase of the cutting efforts and, due to the geometry of this chipping, the feed force was strongly affected. If the cutting efforts of the new cutting tool (VB_{max} = 0 mm) are compared with the worn cutting tool (VB_{max} = 1.071 mm), an increase by 100.9% (412.3 N) can be verified in the cutting force, 423.8% (713.7 N) in the feed force, and 198.9% (319.3 N) in the thrust force when using the worn cutting tool.

According to Fig. 13, the cutting tool used in dry turning with cutting speed of 400 m/min showed a VB_{max} equal to 0.772 mm, generated by the attrition between the workpiece and the tip of the cutting tool, besides the presence of a crater on the rake surface of the tool. Thus, according to Figs. 14 and 15, this wear promoted the increase in the cutting efforts, with the abrasion at the tip of the tool being the major responsible for the generation of a greater friction between the tool and the workpiece, verified by the high increase of the thrust force. If the cutting efforts of the new cutting tool (VB_{max} = 0 mm) are compared with the worn cutting tool (VB_{max} = 0.772 mm), an increase by 23.6% (91.2 N) can be verified in the cutting force, 132.8% (195.8 N) in the feed force, and 211.0% (307.8 N) in the thrust force when using the worn cutting tool.

According to Fig. 20, the cutting tool used in dry turning with cutting speed of 600 m/min showed a VB_{max} equal to 0.481 mm, generated by the attrition between the workpiece and the tip of the cutting tool, besides the presence of crater on the rake surface of the tool. Thus, according to Figs. 21 and 22, it can be verified that this wear promoted the increase in

the cutting efforts. However, this increase was much smaller than the cutting efforts verified for the other cutting conditions studied. It is believed that the abrasion at the tip of the tool was the major responsible for the generation of a greater friction between the tool and the workpiece, increasing the feed and thrust forces. If the cutting efforts of the new cutting tool (VB_{max} = 0 mm) are compared with the worn cutting tool (VB_{max} = 0.481 mm), an increase by 17.8% (64.0 N) can be verified in the cutting force, 116.9% (151.0 N) in the feed force, and 112.3% (155.3 N) in the thrust force when using the worn cutting tool.

Thus, it can be supported that the type of wear and the change in the geometry of the tool that this wear promotes greatly influence the cutting efforts. The smallest cutting efforts in turning of API 5L X70 steel with worn cutting tools TNMG 160408-MF (GC 1125) were found with cutting speed of 600 m/min, dry, and with the tip at the cutting tool with an attrition wear (VB_{max} = 0.481 mm), besides the presence of a crater on the rake surface. The values of the cutting efforts for this condition are cutting force of 424.1 N, feed force of 280.2 N, and thrust force of 293.4 N.

3.3 Analysis of surface roughness

Figure 29 shows the values of surface roughness in pattern R_a proportional to the progress of flank wear of TNMG 160408-MF (GC 1125). The turning tests represented by Fig. 29 were carried out with the dry and cold air system, cutting speed of 200 m/min, feed rate of 0.2 mm/rev, and depth of cut of 0.8 mm.

According to Fig. 29, during the progress of VB_{max} in the experiments carried out with the cold air system, the R_a values were lower than the R_a values obtained in dry experiments, except when the tool was new. As mentioned in Fig. 5, the progress of VB_{max} in the cold air system was slower than in dry turning. Thus, it supports the hypothesis that the use of a cold air system improves the workpiece finishing.

For the cutting speed of 200 m/min in both experiments i.e. dry and cold air system, the progress of VB_{max} was due to the notch progression in the clearance surface of the cutting tools. Thus, it can be seen clearly that the increase in notch wear generated an increase in R_a values. It can be considered that in dry turning, the R_a values increased 2.4 times when compared to the new cutting tool and the worn cutting tool (VB_{max} = 0.148 mm). Moreover, when the cold air system was applied, the R_a values increased 1.4 times when compared with the new cutting tool and the worn cutting tool (VB_{max} = 0.196 mm).

The lowest R_a value obtained in dry turning was 1.83 μm for the new cutting tool. On the other hand, the R_a value was 4.77 μm when the cutting tool failed with VB_{max} of 1.071 mm. Considering the turning with the cold air system, the lowest R_a value obtained was 2.01 μm for a VB_{max} of 0.019 mm. However, the highest R_a value was 3.39 μm when the cutting tool presented a VB_{max} of 0.186 mm. Thus, comparing the results of the dry turning and those of the cold air system, it is believed that the decrease in the cutting zone temperature, generated by the use of the cold air system, has contributed to the reduction of the progress of notch wear in the cutting tool. This also resulted in lower R_a surface roughness values for the workpiece.

Figure 30 shows the surface roughness values in the R_a pattern in relation to the progress of flank wear of TNMG 160408-MF (GC 1125). The turning tests represented by Fig. 30 were carried out in dry and cold air systems, with cutting speed of 400 m/min, feed rate of 0.2 mm/rev, and depth of cut of 0.8 mm.

According to Fig. 30, differently from the results for the cutting speed of 200 m/min, for the cutting speed of 400 m/min it can be seen that the experiments carried out with dry conditions showed R_a values lower than the experiments with the cold air system, except when the tool reached its end of life. For the cutting speed of 400 m/min, in both experiments i.e. dry and cold air system, the progress of VB_{max} was due to

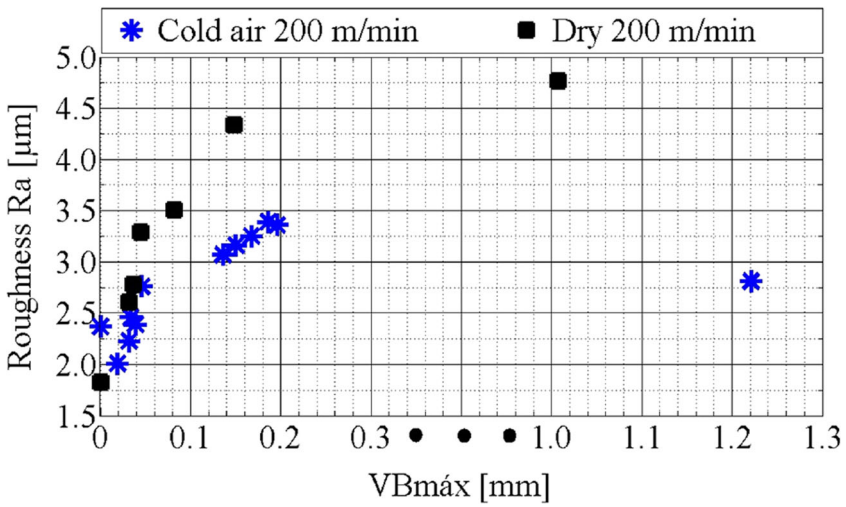

Fig. 29 R_a surface roughness vs. VB_{max} in turning with cutting speed of 200 m/min

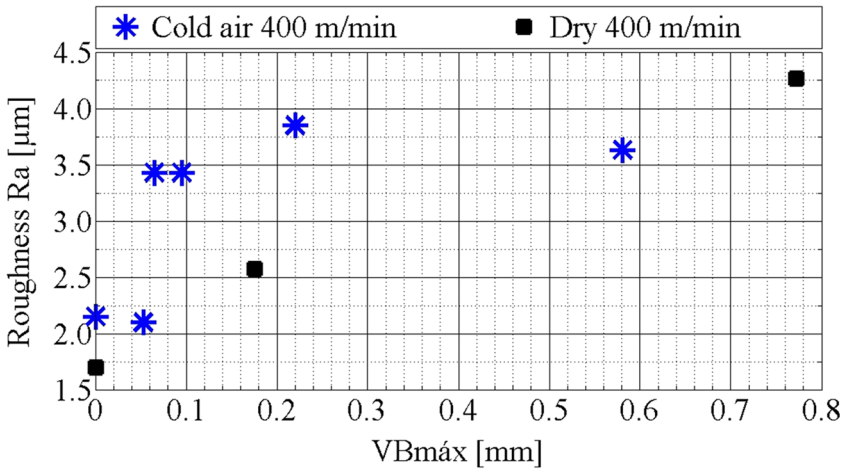

Fig. 30 R_a surface roughness vs. VB_{max} in turning with cutting speed of 400 m/min

the progression of abrasive wear in the tip of the cutting tools. However, in turning tests with the cold air system, there was also the action of the adhesion wear mechanism. Thus, it is believed that the machined material which adhered to the cutting tool changed the geometry of the tool providing a poor surface finish on the workpieces.

It can be seen that the increase in the flank wear promoted a tendency to increase the R_a surface roughness values. In dry turning tests, the R_a values increased 1.5 times when the new cutting tool was compared with the worn cutting tool (VB_{max} = 0.175 mm). In turning with the cold air system, the R_a values increased 1.8 times when the new cutting tool was compared with the worn cutting tool (VB_{max} = 0.220 mm).

According to Fig. 30, the lowest R_a value obtained in dry turning was 1.70 µm, when the cutting tool was new. Yet, the highest R_a value was 4.27 µm when the cutting tool reached a VB_{max} of 0.772 mm. In turning tests with the cold air system, the lowest R_a value obtained was 2.10 µm, when the cutting tool presented a VB_{max} of 0.053 mm. On the other hand, the highest R_a value was 3.85 µm when the cutting tool presented a VB_{max} of 0.220 mm.

Thus, it can be seen that, for new cutting tools, the experiments carried out with cutting speed of 400 m/min presented lower R_a values than experiments carried out with cutting speed of 200 m/min. In dry turning tests, the R_a values for the cutting speed of 200 and 400 m/min were 1.83 and 1.70 µm, respectively. Furthermore, in turning tests with the cold air system, the R_a values for the cutting speeds of 200 and 400 m/min were 2.37 µm and 2.15 µm respectively.

Thus, knowing that the attrition was the main wear mechanism to act in the cutting tools with the cutting speed of 400 m/min, it can be concluded that the decrease in temperature in the cutting zone occurred due to the cold air system. In addition, it promoted the action of the adhesion wear mechanism resulting in higher R_a roughness values for the workpiece.

Figure 31 shows the surface roughness values in the R_a pattern in relation to the progress of flank wear of TNMG 160408-MF (GC 1125). The turning tests represented by Fig. 28 were carried out with the dry and cold air system, cutting speed of 600 m/min, feed rate of 0.2 mm/rev, and depth of cut of 0.8 mm.

According to Fig. 31, the experiments carried out with the cold air system showed R_a values lower than those with the dry system, except when the tool was new. As aforementioned, the progress of VB_{max} in turning tests with the cold air system was slower than in dry turning, which improves significantly the workpiece finish.

For the cutting speed of 600 m/min in both experiments i.e. dry and cold air system, the progress of VB_{max} was due to the abrasive wear in the tip of the cutting tools. Thus, it can be seen that the increase in the flank wear provided a tendency to increase the R_a workpiece surface roughness. In dry turning, the R_a values increased 2.7 times when the new cutting tool is compared with the worn cutting tool (VB_{max} = 0.481 mm). In turning tests with the cold air system, the R_a values were almost the same when the new cutting tool is compared with the worn cutting tool (VB_{max} = 0.488 mm). For the new cutting tool, the R_a value was 2.61 µm, and for the VB_{max} of 0.488 the R_a value was 2.68 µm.

According to Fig. 31, the lowest R_a value obtained in dry turning was 1.93 µm for the new cutting tool. On the other hand, the highest R_a value was 5.12 µm when the cutting tool reached its end of life (VB_{max} = 0.481 mm). In turning tests with the cold air system, the lowest R_a value obtained was 1.89 µm when the cutting tool presented a VB_{max} of 0.075 mm. Furthermore, the highest R_a value was 2.68 µm when the cutting tool presented a VB_{max} of 0.488 mm.

Analysing the influence of the cutting speed for the new cutting tools, it can be seen that the experiments carried out with the cutting speed of 600 m/min presented values for surface roughness in R_a higher than experiments carried out with the cutting speed of 400 m/min. In dry turning tests, the

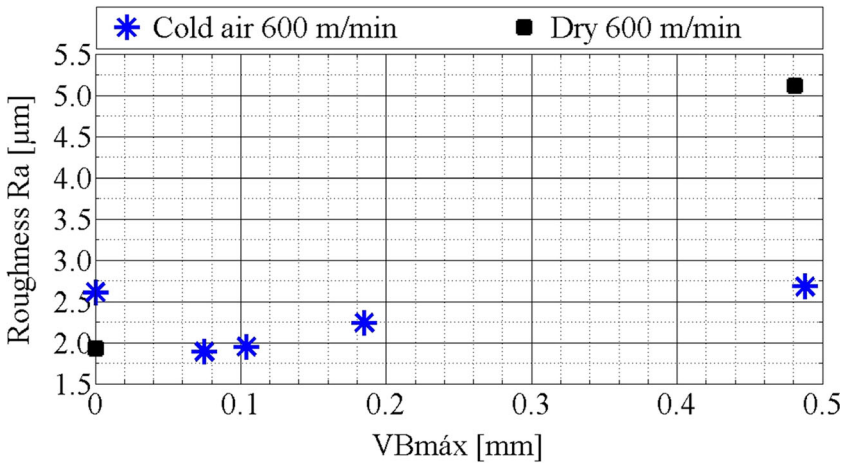

Fig. 31 R_a surface roughness vs. VB_{max} in turning with cutting speed of 600 m/min

R_a values for the cutting speeds of 400 and 600 m/min were 1.70 and 1.93 µm, respectively. On the other hand, in turning tests with the cold air system, the R_a values for the cutting speeds of 400 and 600 m/min were 2.15 and of 2.61 µm, respectively. Thus, it can be affirmed that the increase of cutting speed was sufficient to increase the vibration in the group machine-tool/workpiece/clamping devices, which might have caused the increase of R_a roughness in the workpiece.

Based on what have been exposed about the variation of R_a surface roughness and the evolution of flank wear (VB_{max}) for the traditional cutting speed of 200 m/min, it can be defined that the R_a surface roughness of the workpiece presented an increase with the increase of notch wear that was predominant in this cutting speed. However, for the high cutting speeds of 400 and 600 m/min, the experiments carried out with dry turning tests presented a tendency to increase the R_a surface roughness with the increase of flank wear (VB_{max}). On the other hand, in the experiments carried out with the cold air system, it was not possible to identify any tendency for R_a roughness related with the increase of flank wear (VB_{max}), since, in some cases an increase in R_a values occurred and in other cases a reduction.

4 Conclusions

The main conclusions about the use of high-speed cutting in turning of API 5L X70 steel are as follows:

- The use of a cold air system provided an increase in tool life by 21.8% considering the traditional speed of 200 m/min. On the other hand, the increase was 5.2 and 31.7% for the cutting speeds of 400 and 600 m/min, respectively.
- The use of high cutting speeds provided a significant reduction in tool life. In dry turning, the cutting speeds of 400 and 600 m/min reduced the tool life 18 times and 111 times, respectively. On the other hand, the turning process with the cold air system and with the cutting speeds of 400 and 600 m/min reduced the tool life 21 and 103 times, respectively.
- In dry turning with the cutting speed of 200 m/min, the types of wear were notch and crater wear, with subsequent abrupt failure (chipping). For the high cutting speeds of 400 and 600 m/min, the types of wear observed were flank wear and crater. Furthermore, the adhesion mechanism for cutting speed of 400 m/min was also presented.
- In turning with the cold air system with cutting speed of 200 m/min, the type of wear observed was a notch, with subsequent abrupt failure (chipping). For high-speed cutting with cold air system (400 and 600 m/min), the types of wear observed were flank and crater wear. Furthermore, the cutting speed of 400 m/min also presented the action of adhesion mechanism.
- Concerning the cutting speed, it was found that their increase provided a reduction in the cutting efforts, both in dry experiments and in experiments with cold air system.
- Concerning the worn cutting tools, it was verified that the type of wear and the geometry of the tool, generated by this wear, had a significant influence in the cutting efforts. Each worn cutting tool presented a different behaviour for the cutting efforts, always being higher than the efforts found for the new cutting tools.
- The smallest cutting efforts found for the new cutting tool TNMG 160408-MF (GC 1125) were 356.0 N for cutting force, 120.6 N for feed force and 131.1 N for thrust force, with cutting speed of 600 m/min and using the cold air system.
- The increase of VB_{max} provided the increase in workpiece surface roughness. For turning with the cold air system and cutting speed of 200 m/min, the increase in VB_{max} also provided the increase in surface roughness. However, for high-speed cutting (400 and 600 m/min), it was not possible to identify any tendency for surface roughness.

- The lowest R_a values were obtained with the high-speed cutting of 400 m/min. In dry turning, the R_a value was 1.70 μm and with the cold air system the R_a value was 2.15 μm.

References

1. Acayaba GMA, Escalona PM (2015) Prediction of surface roughness in low speed turning of AISI316 austenitic stainless steel. CIRP J Manuf Sci Technol 11:62–67
2. Beno J, Manková I, Vrabel M, Kottfer D (2013) Roughness measurement methodology for selection of tool inserts. Measurement 46:582–592
3. Selvaraj DP, Chandramohan P, Mohanraj M (2014) Optimization of surface roughness, cutting force and tool wear of nitrogen alloyed duplex stainless steel in a dry turning process using Taguchi method. Measurement 49:205–215
4. Kumar A, Sahoo B (2013) A comparative study on performance of multilayer coated and uncoated carbide inserts when turning AISI D2 steel under dry environment. Measurement 46:2695–2704
5. Aneiro, F. M.; Coelho, R.T.; Brandão, L. C. Turning hardened steel using coated carbide at high cutting speeds. J Braz Soc Mech Sci Eng, 30, 104–109, 2008
6. Katama Y, Obikawa T (2007) High speed MQL finish-turning of Inconel 718 with different coated tool. J Mater Process Technol 192/193:281–286
7. Shaw MC (2004) Metal cutting principles. Oxford University, Oxford 651 p
8. El-Wardany TI, Kishawy HA, Elsbestawi MA (2000) Surface integrity of die material in high-speed hard machining. Part 1.Micrographical analysis. J Manuf Sci Eng 122/4:620–631
9. Pawade RS, Suhas SJ, Brahmankar PK (2008) Effect of machining parameters and cutting edge geometry on surface integrity of high-speed turned Inconel 718. Int J Mach Tools Manuf 48:15–28
10. Akbar F, Matvinga PT, Sheikh MA (2008) An evaluation of heat partition in the high-speed turning of AISI/SAE 4140 steel with uncoated and TiN-coated tools. Proc Inst Mech Eng B J Eng Manuf 222:759–771
11. Abou-El-Hossein KA, Yahya Z (2005) High-speed end-milling of AISI 304 stainless steels using new geometrically developed carbide inserts. J Mater Process Technol 162/163:596–602
12. Brandão LC, Coelho RT, Rodrigues AR (2007) Experimental and theoretical study of workpiece temperature when end milling hardened steels using (TiAl)N-coated and PcBN-tipped tools. J Mater Process Technol 99:234–244
13. Kang MC, Kim KH, Shin SH (2008) Effect of the minimum quantity lubrication in high-speed end-milling of AISI D2 cold-worked die steel (62 HRC) by coated carbide tools. Surf Coat Technol 202/22–23:5621–5624
14. Qehaja N, Jakupi K, Bunjaku A, Bruçi M, Osmani H (2015) Effect of machining parameters and machining time on surface roughness in dry turning process. Proc Eng 100:135–140
15. Upadhyay V, Jain PK, Mehta NK (2013) In-process prediction of surface roughness in turning of Ti-6Al-4V alloy using cutting parameters and vibration signals. Measurement 46:154–160
16. Aslantas K, Ucun I, Çicek AC (2012) Tool life and wear mechanism of coated and uncoated Al2O3/TiCN mixed ceramic tools in turning hardened alloy steel. Wear 274/275:442–451
17. Karpuschewski B, Konrad Schmidt K, Beno J, Maňková I, Frohmüller R, Prilukova J (2015) An approach to the microscopic study of wear mechanisms during hard turning with coated ceramics. Wear 342/343:222–233
18. Attanasio A, Ceretti E, Giardini C (2013) Analytical models for tool wear prediction during AISI 1045 turning operations. Proc CIRP 8:218–223
19. Cantero JL, Díaz-Alvarez J, Miguélez MH, Marín NC (2013) Analysis of tool wear patterns in finishing turning of Inconel 718. Wear 297:885–894
20. Kumar NS, Shetty A, Shetty A, Ananth K, Shetty H (2012) Effect of spindle speed and feed rate on surface roughness of carbon steels in CNC turning. Proc Eng 38:691–697
21. API SPECIFICATION 5L (2000) Specification for Line Pipe. American Petroleum Institute, Washington
22. Settineri L, Faga MG, Lerga B (2008) Properties and performances of innovative coated tools for turning inconel. Int J Mach Tool Manu 48:815–823
23. Sadik MI (2012) Wear development and cutting forces on CBN cutting tool in Hard Part turning of different hardened steels Proc CIRP 1:232–237
24. Chinchanikar, S., Choudhury, S. K., 2013. Wear behaviors of single-layer and multi-layer coated carbide inserts in high speed machining of hardened AISI 4340 steel. J Mech Sci Technol 27:1451–1459.
25. Abukhshim NA, Mativenga PT, Sheikh MA (2005) Investigation of heat partition in high speed turning of high strength alloy steel. Int J Mach Tools Manuf 45:1687–1695
26. LIMA JG, Ávila RF, Abrão AM, Faustino M, Davim JP (2005) Hard turning: AISI 4340 high strength low alloy steel and AISI D2 cold work tool steel J Mater Process Technol 169: 388–395
27. Pawade RS, Joshi SS, Brahmankar PK, Rahman M (2007) An investigation of cutting forces and surface damage in high-speed turning of Inconel 718 J Mater Process Technol 192/193: 139–146
28. Khan MMA, Mithu, MAH, Dhar NR (2009) Effects of minimum quantity lubrication on turning AISI 9310 alloy steel using vegetable oil-based cutting fluid J Mater Process Technol 209:5573–5583